

# Intraburst versus interburst locking in networks of driven nonidentical oscillators

Jack Waddell

*Department of Physics, University of Michigan, Ann Arbor, Michigan 48109, USA*

Michal Zochowski

*Department of Physics, Biophysics Research Division, University of Michigan, Ann Arbor, Michigan 48109, USA*

(Received 24 May 2007; revised manuscript received 1 August 2007; published 30 November 2007)

We investigate the effect of common periodic drive applied to mean-field coupled oscillators and observe a specific realization of synchronization for particular ranges of drive frequency. This synchronization occurs when the phase difference variability between a pair of oscillators on a given cycle is larger than that between consecutive cycles. This synchrony may have implications for neural systems, in which case the apparent locking between neurons based on the magnitude of their interspike intervals may not be consistent with their dynamical locking.

DOI: [10.1103/PhysRevE.76.056216](https://doi.org/10.1103/PhysRevE.76.056216)

PACS number(s): 05.45.Xt, 05.45.Tp, 87.19.La

## I. INTRODUCTION

The past decade has seen engaged investigation of synchronization of chaotic oscillators, but while the synchronization of coupled oscillators [1–9] or driven oscillators [10–13] has been thoroughly examined, these two processes have rarely been applied simultaneously to nonidentical oscillators. Individually, these processes lead to one of five types of synchronization, depending on the degree of coupling or the amplitude and frequency of the drive: Complete or global synchronization, in which the trajectories of two or more oscillators are identical [14,15]; phase synchronization, in which the difference in phases between two oscillators is locked [1,8,16]; lag synchronization, in which the trajectory of one oscillator matches that of another, but lagged by some constant time [2]; cluster synchronization, in which groups of oscillators synchronize to one another within, but not between, the groups [17–19]; and generalized synchronization, in which a mapping can be established between one trajectory and another [20,21].

Herein we study the effect of a common periodic drive applied to a network of diffusively coupled nonidentical oscillators, and observe a realization of phase-lag synchronization in which phases on the same oscillatory cycle are more variable than on the consecutive cycles (a similar phenomenon was observed before in discrete time bursters [22]). To show this, we define a phase event (a Poincaré section crossing). It is known that elements with sufficient coupling or drive have a tendency to synchronize and have events over a short interval compared to the interval between events [15,23–25]. This group of nearly coincident events is here referred to as a population burst (Fig. 1). Here we show that interburst phase variability of those events is smaller than that of intraburst phases. That is, a significant number of oscillators exhibit intercycle locking versus the typically observed intracycle locking.

## II. DETECTION OF TEMPORAL INTERACTIONS IN THE NETWORK OF DRIVEN RÖSSLER OSCILLATORS

We first examine the effects of a near-resonant periodic drive on the dynamics of diffusively coupled, nonidentical

Rössler oscillators given by the following equations:

$$\begin{aligned} \dot{x}_i &= -\omega_i y_i - z_i, \\ \dot{y}_i &= \omega_i x_i + a y_i + \sum_{j=1}^N \frac{\alpha_{ij}}{N-1} (y_j - y_i) + A \sin(\Omega t), \\ \dot{z}_i &= b + (x_i - c) z_i, \end{aligned} \quad (1)$$

where the parameters  $(a, b, c) = (0.15, 0.2, 10)$  are the Rössler parameters,  $N=36$  is the number of oscillators,  $\omega_i = [0.98, 1.02]\omega_0$  is the frequency of oscillator  $i$ ,  $\alpha_{ij}$  is the coupling strength from  $j$  to  $i$ ,  $A=0.5$  is the drive amplitude, and  $\Omega$  is the drive frequency. The parameter  $\omega_0=1$  sets the relative time scale of the dynamics. Herein we consider mean-field coupling, such that  $\alpha_{ij}=\alpha$ .

### A. Measuring asymmetric locking through interevent intervals

We monitor the locking between a pair of oscillators over time by use of causal entropy ( $S^C$ ) [26,27]. Causal entropy is an asymmetric, time-adaptive metric, constructed to detect asymmetric locking between two oscillators based on the intervals between discrete events (e.g., Poincaré section crossings) [28]. They are computed by first constructing two

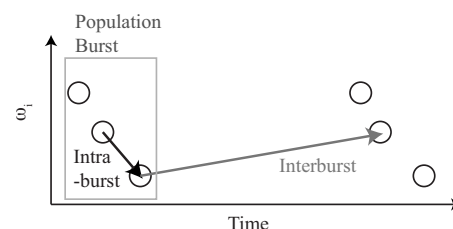


FIG. 1. Schematic of population bursts and intervals for three oscillators. A population burst occurs when most oscillators fire on a cycle. The intraburst interval is the time from the event of the faster oscillator in a population burst to that of the slower. The interburst interval is the time from an event of a slower oscillator in a given population burst to the faster oscillator's event in the next population burst.

time-adaptive histograms of the interevent intervals between the events generated by two oscillators ( $P_{ij}$  and, separately,  $P_{ji}$ ), then calculating the Shannon entropy as a cost estimator of the regularity of the distribution. Until otherwise noted, we define an event for the Rössler oscillators as crossing of the Poincaré section  $z=1, \dot{z}>0$ ; however, the same results are obtained for different Poincaré sections.

Briefly, let  $t_n$  be the time of the  $n$ th Poincaré section crossing for oscillators  $i$  and  $j$ . Also, let  $s_n=\{i,j\}$  indicate the identity of the oscillator that fires at  $t_n$ , and  $\tau_i(n)$  be the last time that oscillator  $i$  fired before  $t_n$ .

At  $t_n$ , we update the histogram  $P_{(s_n)(s_{n-1})}(n)$  by adding  $\Delta_p$  to the bin corresponding to  $t_n - \tau_{s_{n-1}}(n)$ . The histogram is then renormalized by dividing every bin by  $(1+\Delta_p)$ .  $\Delta_p$  is a free parameter which sets the effective length of history of the time-adaptive measure [28]. Note that only consecutive events for a pair of oscillators are taken; that is, those for which  $s_n \neq s_{n-1}$ . This process establishes an exponential attenuation to the memory of the histogram, allowing it to adapt to changes of synchrony as they occur in time. The causal entropy  $S_{(s_n)(s_{n-1})}^C(n) = -\sum_k P_{(s_n)(s_{n-1})(k)}(n) \times \ln[P_{(s_n)(s_{n-1})(k)}(n)]$  is then computed, where  $k$  indexes the bins of the histogram.

The critical capacity of causal entropy is the ability to detect asymmetric locking between pairs of oscillators. If oscillator  $i$  regularly has an event shortly after oscillator  $j$ , but  $j$  does not regularly follow  $i$ , then  $S_{ij}^C(n)$  will go to a small value due to the narrow distribution  $P_{ij}(n)$ , while  $S_{ji}^C(n)$  will remain relatively large. Therefore, one may take the causal entropy difference  $\delta_{ij}^C(n) = S_{ij}^C(n) - S_{ji}^C(n)$  to measure the degree and direction of locking between the two oscillators, excluding the cases of periodicity or completely synchronized oscillators where  $S_{ij}^C(n) = S_{ji}^C(n) = 0$ . For a detailed description of the metric and its properties, see [28].

### B. Other measures of synchrony

We utilize three types of measures to characterize the observed dynamics of the system. They are as follows: Expectivity, a metric which uses the causal entropy measurement to determine whether the direction of locking aligns with a prediction based on oscillator frequency (i.e., that a faster oscillators shall lead a slower one [1]); Spearman rank order correlation, which in this case monitors ordering of events of the oscillators within a population burst with respect to their frequency; and synchronization error, which measures the overall degree of synchrony.

The expectivity  $W$  is given by:

$$W = \frac{1}{N(N-1)} \sum_{i,j,i \neq j}^N w_{ij}, \quad (2)$$

where

$$w_{ij} = \begin{cases} 1 & \text{if } (S_{ji}^C - S_{ij}^C)(\omega_j - \omega_i) > 0, \\ -1 & \text{if } (S_{ji}^C - S_{ij}^C)(\omega_j - \omega_i) \leq 0. \end{cases} \quad (3)$$

Thus pairs of oscillators that have the lower frequency oscillator locked following the faster oscillator contribute posi-

tively to the expectivity, but pairs for which the opposite relationship holds detract from the expectivity. This measure is based on a notion that optimally the faster oscillators lead the slower oscillators when they are phase-lag synchronized [1,2], and thus the slower oscillator should be locked to the faster one in terms of their phase-lag variability.

Spearman rank order correlation ( $R$ ) for the  $m$ th population burst

$$R(m) = 1 - \frac{6 \sum_{i=1}^N D_i^2}{N(N^2 - 1)}, \quad (4)$$

where  $D_i$  is the difference between the rank values of oscillator  $i$  for two different sorting criteria. In this case, the events in a population burst are sorted for (a) time of event and (b) frequency of oscillator generating the event. Therefore, a rank order correlation value of one indicates that fast oscillators lead slow oscillators *within a population burst*, a value of negative one indicates the opposite, and a value of zero indicates no average organization. Note that while rank order correlation measures ordering within a population burst, expectivity compares the strength of locking within and between population bursts.

Finally, the synchronization error is given by

$$E(t) = \frac{1}{N(N-1)} \sum_{j>i} \sqrt{(x_j - x_i)^2 + (y_j - y_i)^2 + (z_j - z_i)^2}. \quad (5)$$

High values of the error indicate that trajectories are non-identical.

## III. RESULTS

We examine here the effect of the drive on the coupled system as a function of the drive frequency  $\Omega$  and the coupling strength  $\alpha$ . The previously described measures of synchrony were applied, with the results shown in Fig. 2. We concentrate here on three observed features: Coupling-dependent synchronous states in the 1:1 phase locking region, large changes in synchrony over small changes in drive frequency, and the asymmetry in the expectivity on the right-hand side of the 1:1 phase locking region.

### A. Coupling and synchrony near the 1:1 locking region

Near the 1:1 phase locking region (i.e., when the external drive frequency matches the resonant frequency of the network;  $0.95 \leq \Omega \leq 1.15$ ), in which some or all of the oscillators lock to the drive, synchrony is promoted for weak coupling and suppressed for strong coupling. In the former case, the drive provides a common organizing feature to oscillators that are not synchronized. Thus the drive organizes each oscillator to it, and thereby indirectly organizes the oscillators. For strong coupling, for which synchrony is attained without driving, the effect of the drive is to somewhat reduce synchrony via competition of the oscillators individually trying to lock to the drive and self-organize to the mean field.

Moreover, near this locking region, there are values of drive frequency which promote synchrony relative to the undriven control and values which suppress it (Fig. 3). This

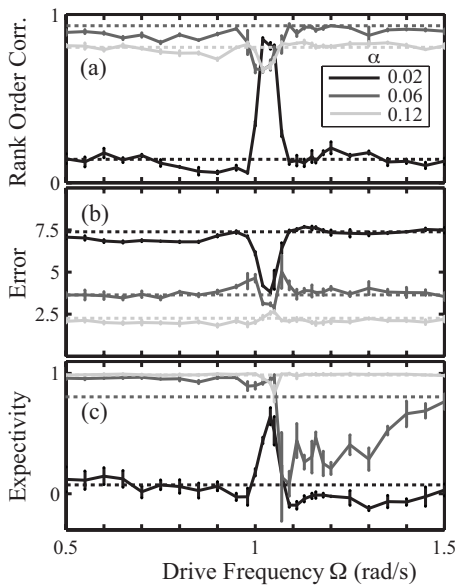


FIG. 2. Effect of drive frequency  $\Omega$  on different measures of synchrony for various coupling strengths  $\alpha=0.02, 0.06, 0.12$  (darker to lighter). The dashed lines represent the values for the undriven control. (a) Rank order correlation and (b) synchronization error. Ordering within population bursts is promoted near the 1:1 locking region for weak coupling, but weakened for stronger coupling. (c) Expectivity. In addition to the changes in synchrony near the 1:1 locking region noted for error and  $R$ , the expectivity reveals substantial asymmetry in locking order on either side of the 1:1 locking frequency.

relatively small variation in driving frequency may lead to very different effects: Synchronization or desynchronization.

### B. Asymmetry of the expectivity metric around the 1:1 locking region

Finally, and most strikingly, we observed prominent asymmetry in the expectivity on either side of the 1:1 frequency locking region (i.e., when  $\Omega$  is below the resonant frequency of the network—*low  $\Omega$  region*—and when  $\Omega$  is above the resonant frequency of the network—*high  $\Omega$  region*). Neither rank order correlation nor error exhibits this asymmetry, indicating that there is a subtle change in the nature of the synchrony on the low- $\Omega$  side relative to the high- $\Omega$  side of the 1:1 locking region. To better capture the asymmetry, we averaged the values of the synchrony measures over frequency ranges  $0.75 \leq \Omega \leq 0.95$  and  $1.15 \leq \Omega \leq 1.35$  (Fig. 4). Both rank order correlation and error are not only symmetric, but near in value to that observed for the undriven case [Figs. 4(a) and 4(b)]. Meanwhile, the expectivity is much higher on the low- $\Omega$  side than on the high- $\Omega$  side [Fig. 4(c)]. The behavior of the undriven control, in which the rise in expectivity is arrested relative to the rise in  $R$ , is due to the development of fragmented groups of oscillators, irrespective of frequency; each group is strongly ordered within itself, but oscillators belonging to different groups are poorly ordered [see Figs. 3(d) and 3(e)].

In Fig. 5 we illustrate the origin of the expectivity in the high- $\Omega$  region using a color-coded map of the causal entropy

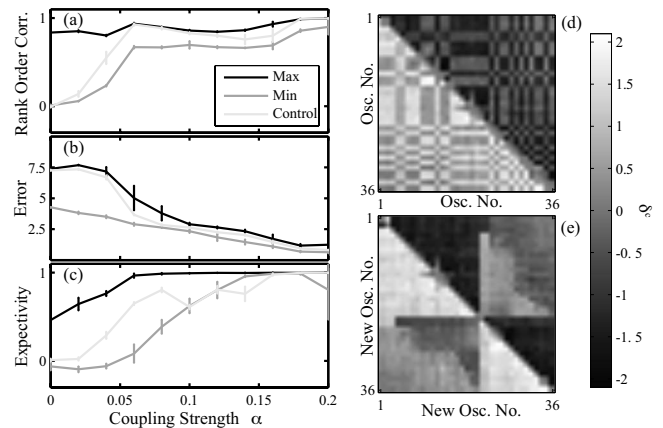


FIG. 3. Extreme values of synchrony measures near 1:1 region largely bound the undriven control values. (a)–(c) From darker to lighter: Maximum, minimum, undriven control; the first two are taken for values over the drive frequency range ( $0.96 \leq \Omega \leq 1.14$ ). For low coupling, there is a wide range of potential values for the synchrony measures over a small drive frequency range. (a) Rank order correlation and (b) synchronization error. The control value is mostly bounded between the maximum and minimum values for the driven system. This suggests variable effects of the drive on the system. (c) Expectivity. Here the control value is reduced for  $0.1 \leq \alpha \leq 0.15$  due to clusterization. This is illustrated for the specific case  $\alpha=0.14$ . (d) Oscillators sorted by frequency  $\omega_i$ . (e) Oscillators clustered with single linkage based on the  $\delta^C$ . Two groups emerge with strong ordering among oscillators within a group but poor ordering between pairs of oscillators of different groups.

difference between all pairs of oscillators, with the oscillators ordered with respect to their frequency  $\omega_i$ . A map resulting in an expectivity [Eq. (3)] near one would be negative above the diagonal and positive below (the maps are anti-symmetric). This can be observed in Fig. 5(a), which illustrates the low- $\Omega$  case. In Fig. 5(b), the high- $\Omega$  case, there is a substantial region of positive values toward the top-right corner. This represents pairs of oscillators for which the lead-lag locking relationship is reversed. However, despite the large number of oscillators in this region of the map, rank order correlation is still quite high. Thus it is not the order of the intraburst events which is switched with these pairs of oscillators, but rather the pattern of the locking between them; these pairs of oscillators exhibit locking that is characterized by the fact that the slower oscillator lags within the population burst, but is weakly locked to the faster one on the same cycle. At the same time this oscillator is strongly locked to, and thus leading, the faster oscillator's event occurring in the next population burst. We will refer to this behavior, smaller interburst variability than intraburst one, as interburst locking.

To further investigate this effect we study a single pair of oscillators from the network (Fig. 6). One can observe that, in this case, the intraburst distribution is somewhat narrowed on the high- $\Omega$  region relative to the low- $\Omega$  region. At the same time the self-interevent events interval (i.e., intervals between events of the same oscillator) distribution is not reduced, indicating that the oscillators themselves are not becoming more periodic. Meanwhile, the distribution of in-

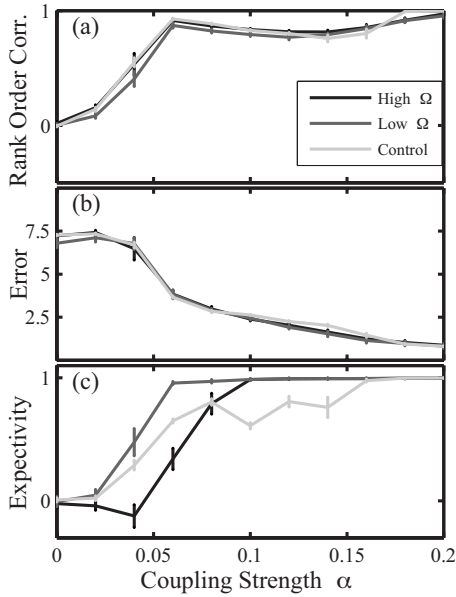


FIG. 4. Detection of symmetric and asymmetric effects around locking region. Measures of synchrony were averaged over the supra-1:1 locking frequency ( $1.15 \leq \Omega \leq 1.35$ ; dark line) and over the sub-1:1 locking frequency ( $0.75 \leq \Omega \leq 0.95$ ; midtone line). This highlights the asymmetry detected by the expectivity. The undriven control value is given by the light line. (a) Rank order correlation and (b) synchronization error. The supra- and sub-1:1 frequency values give the same result, matching the undriven control. (c) Expectivity. The sub-1:1 frequency expectivity is significantly higher than that of the supra-1:1 value. These results indicate that a reversal or weakening of locking between fast and slow oscillators is taking place, but in a way that preserves the order in which they fire.

terevent intervals between the population bursts (i.e., the faster oscillator following the slower) is strongly narrowed. It is this tightening of the interburst distribution that reflects the interburst locking.

To better understand this effect in the network, we examine the variation of the events of the oscillators that occur in each population burst. Here we applied another Poincaré section,  $\phi = 5/4\pi$  [where  $\phi = \arctan(y/x)$ ] to ensure that an event occurs for each oscillator in every population burst. Though the activity of every oscillator was chaotic, the occurrence of population bursts was approximately periodic. We tiled the time line with the population burst period  $T$ , and defined the burst phase (BP) of oscillator  $i$  in population burst  $n$ , which fired at time  $t_i(n)$ , as  $\Phi_i(n) = \{[t_i(n) - T(n-1)]/T\}2\pi$ .

The BPs themselves vary periodically, with a frequency given by the beat frequency between the burst frequency  $\approx \omega_0$  and the drive frequency  $\Omega$  (this periodic variation of the BPs is due to the oscillation of the slow phases [2], the spectrum of which is dominated by the beat frequency). To examine how the relationship between oscillators' BPs affects the asymmetry in the expectivity, we calculated the cross correlation  $X$  between the BPs of pairs of oscillators,

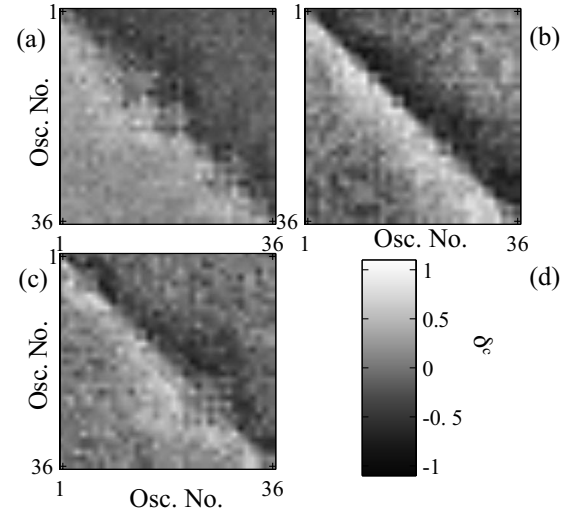


FIG. 5. Reversal of  $\delta^C$  for dissimilar oscillators underlies the asymmetry in expectivity around the 1:1 locking region. Causal entropy difference ( $\delta^C$ ) maps for  $\alpha=0.06$  reveal a reversal of  $\delta^C$  for dissimilar oscillators underlies the reduced expectivity. Oscillators are sorted by frequency  $\omega_i$ . (a)  $\Omega=0.85$ , high expectivity case. (b)  $\Omega=1.25$ , low expectivity case. (c) Undriven control, with high expectivity. (d) Color scale for maps. Panel (b) reveals the reversal of the  $\delta^C$  for pairs of oscillators with large frequency difference (e.g., top right area of map).

$$X_{ij}(\nu) = \frac{\sum_n [\Phi_i(n + \nu) - \mu_i][\Phi_j(n) - \mu_j]}{\sigma_i \sigma_j},$$

where  $\nu$  is the lag shift (in units of population burst period), and  $\mu_i$  and  $\sigma_i$  are the mean and standard deviation of  $\Phi_i$  over time.

The cross correlations were calculated for pairs of oscillators  $i$  and  $j$  such that  $\omega_i > \omega_j$ . The pairs were divided into two categories, those which contribute positively to the expectivity and those which contribute negatively [see Eq. (3)]. The cross correlations of the BPs of these two groups were averaged; Fig. 7 shows the results. This analysis reveals the governing factor: Pairs that contribute positively to the expectivity have cross correlations of BPs peaked at zero lag, while pairs that contribute negatively to the expectivity have cross correlations peaked at a lag of one population burst period. Thus we have observed interburst locking using two approaches: The variation of the inter- and intraburst intervals and the high correlation between burst phases of the population bursts.

One distinction between intra- and interburst locking is the average frequency of the slow phases. The slow phase  $\Theta_i$  of an oscillator is found by subtracting the linear component of the unwrapped phase  $\phi_i$ , i.e.,  $\Theta_i = \phi_i - \omega_i t$ , where  $\omega_i$  is the observed frequency of the oscillator (in this regime locked such that  $\omega_i = \omega$  for all oscillators). The spectrum of the slow phase has a large component at the beat frequency  $\Omega - \omega_i$ , but is not locked to this frequency. This is determined by examining the oscillatory progression of the slow phase by taking the Hilbert transform,  $\hat{s}(t) = (1/\pi) \int_{-\infty}^{\infty} [s(\tau)/(t-\tau)] d\tau$ , where  $s(\tau)$  is the slow phase signal. The average frequency of os-

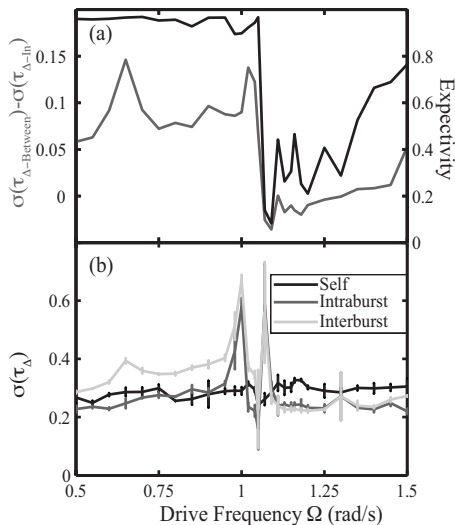


FIG. 6. Standard deviation of interspike interval distribution between the fastest and slowest oscillators further illustrates the interburst locking. (a) (Gray line) Difference between the standard deviation of the interburst distribution  $\sigma(\tau_{\Delta\text{-between}})$  and the standard deviation of the intraburst distribution  $\sigma(\tau_{\Delta\text{-within}})$  and (black line) the expectancy. The  $\sigma$  difference aligns with the expectancy, indicating the origin of the drop in the latter. (b) The standard deviation  $\sigma$  of the distribution of interspike intervals  $\tau_{\Delta}$ : Between an oscillator's own events (black line); between the leading oscillator in a population burst and a following oscillator ("in burst"; midtone line); and between a slow oscillator and a fast oscillator firing in the next population burst ("in-between burst;" light line). While the oscillators do not become more periodic (the self-ISI distribution does not change), the interburst distribution becomes narrower for drive frequency above the 1:1 region.

cillation of the slow phases is shown in Fig. 8. The significant difference in the frequency of the slow phase oscillations for the interburst and intraburst regimes may indicate clues for the modes of oscillation that result in these synchronies.

This interburst locking appears mostly between the oscillator pair that has a relatively large frequency difference,  $\delta\omega$  [see Fig. 7(c)], and is characterized by a relatively high synchronization error (precluding complete synchronization), a high rank order correlation, and a low or negative expectancy.

### C. Neuronal systems

Interburst locking may hold significant implications for our understanding of neural activity in the brain. Neural oscillations are ubiquitous in the brain, and are considered important to its function. For example, the theta rhythm (at frequency 4–8 Hz) and gamma rhythm (30–80 Hz) are particularly important in the hippocampus. These rhythms facilitate communication and may be critical in memory management [29,30]. They are also thought to organize the order of neuron activity within a population burst. Interburst locking may alter this view, suggesting that a periodic signal can order the neurons between bursts as well.

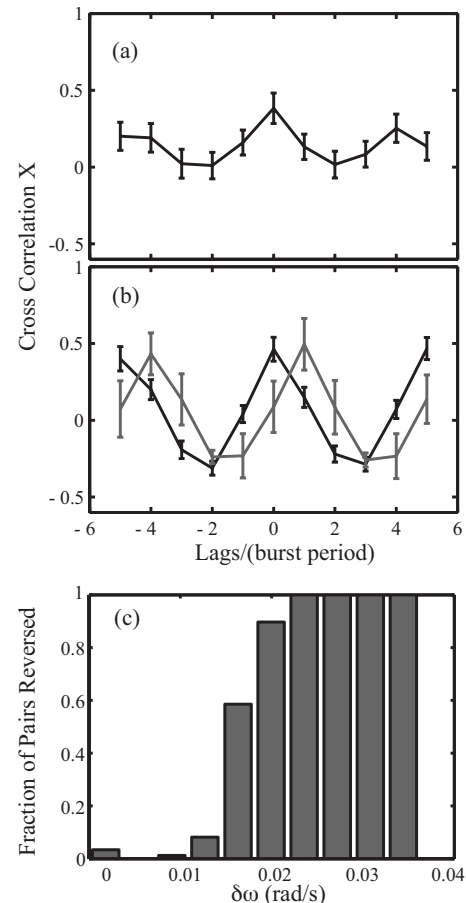


FIG. 7. Cross correlation of the burst phase (BP). The black line is for pairs of oscillators that contribute positively to the average expectancy. The lighter line is for pairs that contribute negatively [i.e., as per Eq. (3)]. [Note: In panel (a), only pairs that contribute to expectancy exist.] (a)  $\Omega=0.9$ , the high expectancy case, demonstrating only intraburst locking. (b)  $\Omega=1.25$ , the low expectancy case, which demonstrates both intra- and interburst locking. The cross correlation for expectancy-detracting pairs is strongly peaked at lag=1, showing that the BP of the slow oscillator correlates strongly to the BP of the fast oscillator in the next population burst. The positive expectancy-contributing pairs in both (a) and (b) are peaked at lag=0, indicating that the BPs of the faster and slower oscillators in these pairs vary together in the same population burst. (c) A histogram of the fraction of pairs of oscillators which exhibit interburst locking (i.e., contribute negatively to expectancy) as a function of their frequency difference. Oscillator pairs with very small frequency exhibit both intra- and interburst locking, whereas oscillator pairs with relatively large frequency differences exhibit predominantly interburst locking.

We believe that intraburst locking will require coherence to the driving signal. Pyramidal cells in CA1 are known to have a subthreshold resonance with the theta rhythm [30] which may establish such a coherence. Other neurons in the brain may have similar resonances to this or other frequency bands. For example, the gamma rhythm is known to be important to the activity of hippocampal interneurons, and thus it is possible that a resonance exists in those cells to that band.

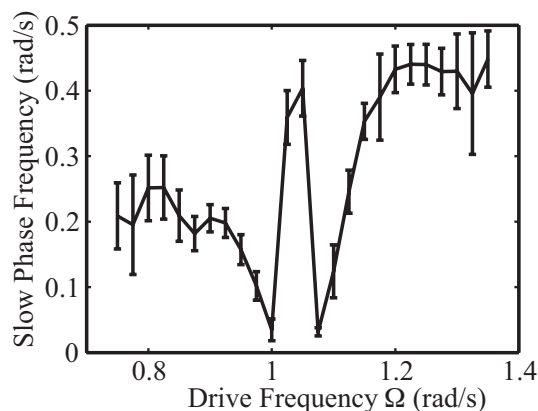


FIG. 8. Average frequency of the slow phases. The slow phases on the low- $\Omega$  side progress more slowly than those on the high- $\Omega$  side. This distinction may underlie the intraburst locking observed in the case of high- $\Omega$  driving.

To see whether this phenomenon could be observed in neural systems, we also investigated a network of Hindmarsh-Rose model neurons with diffusive (electrical) coupling, which is common in the hippocampus between interneurons and may exist between pyramidal cells in CA1 and CA3 [31].

There is good evidence that chaotic behavior appears in some neural systems [32–34]. However, the degree to which chaotic behavior exists in neurons in the brain is still a matter of much discussion [35]. The search for chaos in the brain is motivated by the observation of rich dynamical behaviors, such as complex forms of synchronization [36,37], that not known in simpler nonlinear systems. These behaviors have also motivated the development of numerous neuronal models. Here we utilize one of these models, the Hindmarsh-Rose neuron, to determine whether intraburst locking can be observed in such a model neuronal system.

The Hindmarsh-Rose system is given by the following equations:

$$\begin{aligned} \dot{x}_i &= y_i + 3x_i^2 - x_i^3 - z_i + I_{0i} + \sum_{j=1}^N \frac{\alpha_{ij}}{N-1} (x_j - x_i) + A \sin(\Omega t), \\ \dot{y}_i &= 1 - 5x_i^2 - y_i, \\ \dot{z}_i &= 0.006[4(x_i + 1.6) - z_i], \end{aligned} \quad (6)$$

where  $I_{0i}=[3.07, 3.33]$  is the input current, which governs the spiking activity and frequency of the neurons,  $\alpha_{ij}=\alpha$  is the coupling strength from  $j$  to  $i$ ,  $A=1$  is the drive amplitude, and  $\Omega$  is the drive frequency. For the  $S^C$  calculation, the discrete event is taken to be the spike time.

This representation of a neuron shares the common feature with the Rössler oscillator that it has an internal frequency, which is related to the external current parameter  $I_0$ . Figure 9 summarizes the results determined for the Rössler oscillators and presents similar results for the Hindmarsh-Rose system [Eq. (6)]. We find similar interburst locking in the Hindmarsh-Rose oscillators as well.

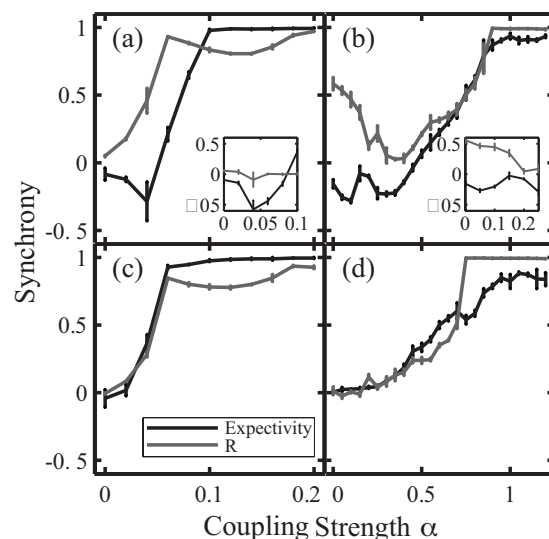


FIG. 9. Interburst locking in the Rössler and Hindmarsh-Rose systems, indicated by the expectivity (dark line) and rank order correlation ( $R$ ; lighter line) vs coupling strength  $\alpha$ . The insets show blown-up portions of the expectivity and  $R$ , minus the values of the undriven control. Panels (a) and (c) show Rössler results, while (b) and (d) show Hindmarsh-Rose (HR) data. Panels (a) and (b) show data for drive frequencies at which interburst locking is observed. Panels (c) and (d) show only intraburst locking. (a) Rössler  $\Omega = 0.85$ . The interburst locking region is  $\alpha \leq 0.06$ . (b) Hindmarsh-Rose minimum values over  $\Omega = [0.04, 0.14]$ . The interburst locking region is for  $\alpha \leq 0.2$ . (c) Rössler  $\Omega = 1.25$ . (d) Hindmarsh-Rose minimum values over  $\Omega = [0.14, 0.2]$ .

#### IV. CONCLUSIONS

We have identified a subtle realization of synchrony, in which the locking between a slow oscillator and a fast oscillator is reversed from that implied by merely the magnitude of their interevent intervals. This synchronization is characterized by a lack of intraburst locking but high interburst locking observed in some oscillatory pairs. In this paper, this phenomenon exemplifies itself by a high synchronization error, high rank order correlation, and reduced expectivity. We believe that our results are generic and will appear in systems in which a phase can be defined that is coherent to the phase of the drive and may underlie formation of long term correlations in the system. The cause of this locking remains elusive, though the cross correlation of the burst phases and the frequency difference of the slow phase oscillation suggest that the origin of the behavior lies in the slow phases of the oscillators, as the former are merely a coarse graining of the latter. It may be that higher-order phase locking exists in these slow phases in certain modes of oscillation. The symmetry of the modes around the resonant frequency of the oscillators is broken by some unknown means.

This form of synchrony leads to a counterintuitive suggestion. The locking relationship between a pair of oscillators (or neurons) might not always be captured by comparing the magnitude of the interevent intervals between them. Indeed, while one oscillator may follow another in any given population burst, it might be more accurate to consider it leading

its purported leader in the next population burst. Should this synchrony exist in *in vivo* neural systems as well, it leads to an even more counterintuitive notion. While it is known that the first neuron to fire in a population burst is not necessarily causing those following it to fire, it may be that the laggards in a population burst are in fact setting the phase of the population burst leaders firing in the next population burst to follow.

## ACKNOWLEDGMENTS

This research was done with the support of the National Institutes of Health (1 R21 EB003583) (M.Z.) and NIH Molecular Biology Training Grant (2T32GM08270-17) (J.W.). The authors would like to thank the Center for the Study of Complex Systems at the University of Michigan for the use of their computer systems for this investigation.

- 
- [1] M. G. Rosenblum, A. S. Pikovsky, and J. Kurths, *Phys. Rev. Lett.* **76**, 1804 (1996).
- [2] M. G. Rosenblum, A. S. Pikovsky, and J. Kurths, *Phys. Rev. Lett.* **78**, 4193 (1997).
- [3] A. S. Pikovsky, M. G. Rosenblum, and J. Kurths, *Europhys. Lett.* **34**, 165 (1996).
- [4] S. J. Baek and E. Ott, *Phys. Rev. E* **69**, 066210 (2004).
- [5] S. G. Guan, C. H. Lai, and G. W. Wei, *Phys. Rev. E* **72**, 016205 (2005).
- [6] Z. H. Liu and B. Hu, *Int. J. Bifurcation Chaos* **11**, 3137 (2001).
- [7] E. Ott, P. So, E. Barreto, and T. Antonsen, *Physica D* **173**, 29 (2002).
- [8] J. W. Shuai and D. M. Durand, *Phys. Lett. A* **264**, 289 (1999).
- [9] Z. G. Zheng and C. S. Zhou, *Commun. Theor. Phys.* **37**, 419 (2002).
- [10] A. S. Pikovsky, M. G. Rosenblum, G. V. Osipov, and J. Kurths, *Physica D* **104**, 219 (1997).
- [11] H. Chate, A. Pikovsky, and O. Rudzick, *Physica D* **131**, 17 (1999).
- [12] J. Y. Chen, K. W. Wong, H. Y. Zheng, and J. W. Shuai, *Phys. Rev. E* **63**, 036214 (2001).
- [13] E. H. Park, M. A. Zaks, and J. Kurths, *Phys. Rev. E* **60**, 6627 (1999).
- [14] H. Fujisaka and T. Yamada, *Prog. Theor. Phys.* **69**, 32 (1983).
- [15] L. M. Pecora and T. L. Carroll, *Phys. Rev. Lett.* **64**, 821 (1990).
- [16] M. G. Rosenblum, A. S. Pikovsky, and J. Kurths, *IEEE Trans. Circuits Syst., I: Fundam. Theory Appl.* **44**, 874 (1997).
- [17] K. Kaneko, *Physica D* **41**, 137 (1990).
- [18] V. N. Belykh, I. V. Belykh, and E. Mosekilde, *Phys. Rev. E* **63**, 036216 (2001).
- [19] M. I. Rabinovich, J. J. Torres, P. Varona, R. Huerta, and P. Weidman, *Phys. Rev. E* **60**, R1130 (1999).
- [20] N. F. Rulkov, M. M. Sushchik, L. S. Tsimring, and H. D. I. Abarbanel, *Phys. Rev. E* **51**, 980 (1995).
- [21] L. Kocarev and U. Parlitz, *Phys. Rev. Lett.* **76**, 1816 (1996).
- [22] N. F. Rulkov, *Phys. Rev. Lett.* **86**, 183 (2001).
- [23] A. Pikovsky, M. Rosenblum, and J. Kurths, *Synchronization: A Universal Concept in Nonlinear Sciences* (Cambridge University Press, Cambridge, UK, 2003).
- [24] E. Ott, *Chaos in Dynamical Systems*, 2nd ed. (Cambridge University Press, Cambridge, UK, 2002).
- [25] S. Boccaletti, J. Kurths, G. Osipov, D. L. Valladares, and C. S. Zhou, *Phys. Rep.* **366**, 1 (2002).
- [26] M. Zochowski and R. Dzakpasu, *J. Phys. A* **37**, 3823 (2004).
- [27] R. Dzakpasu and M. Zochowski, *Physica D* **208**, 115 (2005).
- [28] J. Waddell, R. Dzakpasu, V. Booth, B. Riley, J. Reasor, G. Poe, and M. Zochowski, *J. Neurosci. Methods* **162**, 320 (2007).
- [29] G. R. Poe, D. A. Nitz, B. L. McNaughton, and C. A. Barnes, *Brain Res.* **855**, 176 (2000).
- [30] G. Buzsáki, *Neuron* **33**, 325 (2002).
- [31] B. W. Connors and M. A. Long, *Annu. Rev. Neurosci.* **27**, 393 (2004).
- [32] G. Mpitsos, R. Burton, H. Creech, and O. Seppo, *Brain Res. Bull.* **21**, 529 (1988).
- [33] X. Pei and F. Moss, *Nature (London)* **379**, 618 (1996).
- [34] H. Lechner, D. Baxter, J. Clark, and J. Byrne, *J. Neurophysiol.* **75**, 957 (1996).
- [35] H. Korn and P. Faure, *C.R. Biol.* **326**, 787 (2003).
- [36] F. Mormann, K. Lehnertz, P. David, and C. Elger, *Physica D* **144**, 358 (2000).
- [37] P. Tass, M. G. Rosenblum, J. Weule, J. Kurths, A. Pikovsky, J. Volkmann, A. Schnitzler, and H.-J. Freund, *Phys. Rev. Lett.* **81**, 3291 (1998).